THE ASTROPHYSICAL JOURNAL, 248:569–583, 1981 September 1

THE OPTICAL AND ULTRAVIOLET SPECTRUM OF THE PLANETARY NEBULA NGC 2440

G. A. SHIELDS[a]
Department of Astronomy, University of Texas at Austin
L. H. ALLER AND C. D. KEYES
Department of Astronomy, University of California, Los Angeles
AND
S. J. CZYZAK
Department of Astronomy, Ohio State University
Received 1980 October 6; accepted 1981 March 11

ABSTRACT

New measurements of the optical and ultraviolet emission-line intensities of the high-excitation planetary nebula NGC 2440 in the wavelength range 1240–8578 Å are analyzed with the aid of photoionization models. The observed [O III] and [N II] temperatures (13,800 K and 10,000 K, respectively) differ by more than the models predict. Inclusion of charge-transfer reactions at published rates improves agreement between calculated and observed abundances of many ions, but worsens the agreement for several highly ionized ions. Nitrogen shows a larger overabundance $N(\mathrm{N})/N(\mathrm{O}) \approx 1.0$, whereas ultraviolet lines give a carbon abundance close to the solar value. The refractory elements magnesium, calcium, and iron have similar gas-phase depletions of ~ 1.5 dex. The abundances of oxygen, neon, sodium, sulfur, chlorine, potassium, and argon are roughly solar.

Subject headings: nebulae: abundances — nebulae: individual — nebulae: planetary — ultraviolet: spectra

I. INTRODUCTION

The high-excitation planetary nebula (PN) NGC 2440 is interesting because of its rich, high-excitation emission-line spectrum, its complex morphology, and its exceptionally strong [N II] lines. Minkowski (1964) presents photographs of NGC 2440 at various exposures and remarks that it is "an example of an object so complicated it defies description." Curtis (1918) describes a core with two condensations separated by 7″. The main body of the nebula is contained within a radius of about 10″, and the faint envelope extends to about 30″ radius. Kaler and Aller (1974) conclude that the bright inner nebula is expanding faster than the halo.

Early spectral studies include those by Wyse (1942) and Aller (1951), and more recent investigations include those by Aller (1957), Osterbrock (1960), Kaler (1966), Aller, Czyzak, and Kaler (1968), Aller and Walker (1970), and Peimbert and Torres-Peimbert (1977). These studies indicate an electron density $N_e \approx 10^{3.5}$ cm^{-3} in the bright core of the nebula, decreasing to as low as 600 cm^{-3} at a position 14″ NE of center. The [O III] and [N II] temperatures are $\sim$13,500 K and 10,000 K, respectively. In keeping with the complex morphology, the ionization structure is highly stratified, as exemplified by the fluctuations in the intensity of [N II] and especially [N I]. This stratification is shown strikingly in spectra secured by Aller and Walker (1970) with the electronic camera. (See their Fig. 4).

We have carried out a detailed study of the emission-line spectrum of NGC 2440 with several goals in mind. Modern electronic spectrophotometers allow one to measure line intensities accurately, recalibrate earlier photographic spectra which give intensities for many faint lines, and extend the spectral coverage to longer wavelengths. Ultraviolet (UV) line intensities are obtainable with the *IUE* satellite, and these observations are especially interesting for NGC 2440 because of its wide range of ionization. The UV lines of C III] and C IV are important because of the uncertain indications of very high carbon abundances in planetary nebulae based on optical permitted lines. In an attempt to extract the maximum information from the spectrum, we have constructed a photoionization model for this object. The model gives us ionization corrections to derive abundances for the many chemical elements represented in our data, and it allows us to assess the importance of the variety of charge-transfer rate coefficients that have recently become available.

II. OBSERVATIONS

For the "optical" wavelength region, we have combined spectral measurements from several sources: (1) the older photographic and photoelectric series of observations summarized by Aller, Czyzak, and Kaler (1968), covering the region shortward of about λ5000; (2) the Lallemand tube data by Aller and Walker (1970) covering the region between λ4600 and λ5900; and (3) new photoelectric scanner results obtained at Mount Wilson and image tube scanner (ITS) data secured with

[a] Alfred P. Sloan Research Fellow.

the Shane telescope at Lick Observatory (1972–1976 "red" tube and 1979 "green" tube).

Ultraviolet observations in the wavelength range λ1240–λ3204 were obtained with the *IUE* satellite on 1979 May 14. Data were obtained with both the short wavelength camera (λ1170–λ1950) and the long wavelength camera (λ1900–λ23500), but only at low dispersion. The entrance aperture was a 10″ × 20″ ellipse oriented in position angle 10°, and this should have captured most of the light from the bright core of the nebula. The observed fluxes were corrected for background radiation contamination by standard NASA reduction procedures and then converted to true fluxes with the aid of the corrected *IUE* instrumental response function.

We corrected the optical region line intensities using essentially Whitford's (1958) extinction curve with a reddening coefficient $C = \Delta \log I(\mathrm{H}\beta) = 0.63$, which brings the observed Balmer decrement into agreement with theoretical values for radiative recombination (Brocklehurst 1971). To estimate the ultraviolet extinction one may compare the observed $I(\lambda1640)/I(\lambda4686)$ and $I(\lambda2734)/I(\lambda4686)$ ratios with theoretical values of 6.85 and 0.218, respectively (Brocklehurst 1972); this procedure gives $C = 0.67$ and 0.68, respectively. For the *IUE* data we employed the reddening curves given by Seaton (1979) and adopted $C = 0.63$. The agreement between the extinction-corrected fluxes in He II λ1640 and O II] λ1662 (see § III) and those expected from the optical lines of these ions provides confirmation that the *IUE* and optical observations represent portions of the nebula having similar conditions of ionization and temperature.

TABLE 1

IUE INTENSITIES[a] FOR NGC 2440

λ	Identification	F	f	I
1239, 1241 ..	N V	3.5 (−12)	1.641	113
1371	O IV]	<6.0 (−13):	1.354	13
1391	Si IV }	2.51 (−12)	1.308	49
1403	O IV] }			
1487	N IV]	1.11 (−11)	1.231	198
1548, 1550 ..	C IV	2.7 (−11)	1.185	454
1640	He II	2.7 (−11)	1.138	413
1661, 1666 ..	O III]	3.0 (−12)	1.130	46
1747	N III]	9.2 (−12)	1.121	140
1883, 1892 ..	Si III]	4.3 (−13):	1.208	7:
1906, 1909 ..	C III]	4.2 (−11)	1.228	752
2326, 2328 ..	C II]	3.4 (−12)	1.319	69
2422	[Ne IV]	8.7 (−12)	1.122	131
2470	[O II]	1.45 (−12)	1.027	19
2511	He II	1.32 (−11)	0.957	16
2734	He II	1.35 (−12)	0.701	11
2784	[Mg V]	0.91 (−12):	0.660	7:
2800	Mg II	0.90 (−12)	0.625	4:
3047	O III	7.2 (−13)	0.496	4.4
3133	O III	9.1 (−12)	0.455	52
3204	He II	3.51 (−12)	0.420	19

[a] Reddening-corrected intensity I on the scale $\mathrm{H}\beta = 100$. Here f is the extinction factor from Seaton 1979; f has a different meaning in Table 2. A colon indicates an uncertainty ≳50%.

Table 1 gives the *IUE* data. Successive columns give the wavelength, the identification, the measured flux (ergs cm^{-2} s^{-1}), the extinction factor from Seaton, f, and finally, the intensity corrected for interstellar extinction, normalized to $I(1640) = 413$, which corresponds to $I(\lambda1640)/I(\lambda4686) = 6.85$.

Table 2 then gives the "optical" region intensities without any reddening correction as well as I_c, the values as corrected with the Whitford data and $C = 0.63$. All line intensities are expressed on the scale $I(\mathrm{H}\beta) = 100$. In the optical region, lines with intensities greater than 5 should be accurate to about 10%. For intensities in the 1–5 range we expect an error of the order of 20%. Lines whose intensities fall in the range 0.5 to 1.0 may be in error by 30–40%, and lines of intensity less than 0.5 have errors of 50% or more. In the *IUE* region, the fluxes should be accurate to about 10% for the strongest lines but the weakest features tabulated may be in error by the order of 50%.

These figures refer to measurement errors and do not address the fact that different techniques refer to different areas of this highly stratified nebula. Although all the ITS data were secured in the brightest part of the southern lobe, the older photographic intensities required more averaging; and the photoelectric data usually include all or most of the nebula. In comparing our result with those of Torres-Peimbert and Peimbert (1977), some differences emerge in the [N II] and [S II] lines. These are of such a nature that they cannot be attributed to a wavelength-dependent effect; one must assume that different parts of the nebula have been measured. The final tabulation of intensities applies for the most part of the southern bright lobe at a distance of about 3″.5 from the nebular center in position angle 135°, but lines that show marked stratification should be interpreted with caution. Since all data longward of λ3700 are derived essentially from the ITS system, these difficulties may manifest themselves in the far-UV and in some weak lines observed only with the Lallemand cell.

III. PHYSICAL CONDITIONS

Our data contain a number of line intensities that reveal the physical conditions at the locations of various ions. Optical line ratios that primarily indicate temperature include [N II] λ6584/λ5755, [O III] λ5007/λ4363, and [Ar III] λ7135/λ5192. Electron density indicators include [O II] λ3729/λ3726, [S II] λ6717/λ6730, and [Cl III] λ5517/λ5537. The ratios [O II] λ3727/λ7325 and [S II] λ4068/λ6730 are sensitive to both temperature and density. Figure 1 shows the constraints on the electron density N_e and temperature T imposed by various line ratios. The analysis was carried out using the values of the collision strengths summarized in the Appendix and five-level computations of the level populations.

For such a complex object, it is no surprise that the curves fail to converge on a single pair of values for N_e and T. Nevertheless, one may reasonably adopt as representative the values $N_e = 3000$ cm^{-3} from [O II] and [S II] along with T(N II) = 10,000 K and T(O III) = 13,800 K.

TABLE 2

OPTICAL EMISSION LINE INTENSITIES FOR NGC 2440

λ	Identi-fication	I_o	f	I_c
3109	[Ar III]	0.44	0.500	0.89
3121	O III	0.37	0.504	0.74
3133	O III	10.6	0.507	20.9
3182		0.40	0.519	0.77
3188	He I	0.88	0.520	1.7
3203	He II	6.86	0.524	13.1
3231 3233	S III S II	0.46	0.531	0.86
3241	[Na IV]	0.75	0.533	1.40
3288	O II	0.10	0.545	0.19
3291	O II	0.15	0.546	0.27
3299	O IV	0.68	0.548	1.25
3312	O III	2.36	0.550	4.3
3341	O III	3.9	0.558	7.0
3343 3346	[Ne III] [Ne V]	17.2	0.558	30.9
3363	O III	0.17	0.564	0.30
3380	O IV	0.44	0.568	0.77
3385	O III O IV	0.29	0.570	0.51
3423	O IV	0.33	0.574	0.57
3409	O IV	0.21	0.575	0.36
3411	O IV	0.29	0.576	0.50
3415	O III	0.16	0.577	0.28
3426	[Ne V]	56	0.580	97
3428	O III	6.1	0.58	10.6
3433	O III	0.17	0.58	0.29
3444	O III	9.4	0.584	16.2
3466	[N I]	0.32	0.590	0.54
3479	N IV, He I	0.20	0.593	0.34
3483	N IV	0.107	0.594	0.18
3487	He I	0.107	0.595	0.18
3499	He I	0.14	0.600	0.23
3531	He I	0.061	0.607	0.10
3544	He I	0.15	0.610	0.24
3568	Ne II	0.10	0.617	0.16
3587	He I	0.17	0.622	0.27
3609	C III	0.033	0.627	0.05
3614	He I	0.057	0.629	0.09
3623		0.82	0.631	0.13
3634	He I	0.17	0.634	0.27
3653	He I	0.14	0.640	0.22
3674	H 23	0.27	0.645	0.42
3676	H 22	0.37	0.646	0.57
3679	H 21	0.42	0.646	0.65
3682	H 20	0.50	0.647	0.77
3686	H 19	0.57	0.648	0.88
3691	H 18	0.66	0.650	1.02
3697	H 17	0.70	0.651	1.07
3704	H 16	0.93	0.653	1.43
3705	He I	0.35	0.653	0.54
3707	O III	0.20	0.654	0.31
3712	H 15	1.08	0.656	1.65
3715	O III	0.16	0.656	0.24
3722	H 14 O III	1.78	0.658	2.7
3727	[O II]	93.7	0.660	142
3734	H 13	1.5:	0.662	2.3:
3750	H 12	1.86	0.665	2.8
3754	O III	0.67	0.668	1.0
3757	O III	0.27	0.670	0.4
3760	O III	2.7	0.670	4.0
3770	H 11	2.7	0.672	4.0
3797	H 10	2.9	0.680	4.3
3835	H 9	4.8	0.688	7.0
3868	[Ne III]	84	0.700	121
3889	H I, He I	11.7	0.707	16.5
3967 3970	[Ne III] H I	37	0.729	51
4009	He I	0.16	0.739	0.22
4026	He I	1.49	0.746	2.0
4068	[S II]	1.96	0.752	3.6
4076	[S II]	0.62	0.752	0.82
4097	N III	1.70	0.758	2.24
4101	Hδ	19.3	0.759	25.4
4143	He I	0.29	0.762	0.38
4199	He I	0.91	0.787	1.16
4227	[Fe V]	0.22	0.794	0.28
4267	C II	0.32	0.806	0.40
4340	Hγ	38.3	0.827	46.3
4363	[O III]	21.7	0.835	26.0
4379	N III	0.20	0.840	0.24
5056	Si II	0.044	1.07	0.041
5092		0.070	1.081	0.065
5131		0.16	1.097	0.15
5146	[Fe VI]	0.10	1.102	0.09
5160	[Fe VII]	0.12	1.108	0.11
5176	[Fe VI]	0.13	1.118	0.12
5192	[Ar III]	0.34	1.120	0.30
5198	[N I]	7.2	1.123	6.4
5200	[N I]	5.6	1.124	5.0
5270	[Fe III]	0.07	1.147	0.06

TABLE 2—*Continued*

λ	Identi-fication	I_o^a	f^b	I_c^c	λ	Identi-fication	I_o^a	f^b	I_c^c
4388	He I	0.40	0.842	0.48	5278	[Fe VII]	0.045	1.150	0.04
4471	He I	2.90	0.868	3.3	5309	[Ca V]	0.09	1.62	0.08
4541	He I	1.86	0.892	2.1	5323	[Cl IV]	0.15	1.170	0.13
4562		0.11	0.898	0.12:	5412	He II	4.9	1.202	4.1
4571	Mg I	0.16	0.902	0.18	5518	[Cl III]	0.63	1.244	0.51
4607	[Fe III]	0.23	0.922	0.25	5538	[Cl III]	0.79	1.249	0.63
4634	N III	2.1	0.920	2.3	5593	O IV	0.21	1.272	0.14
4641	N III	4.5	0.923	4.8	5755	[N II]	17.1	1.337	12.8
4647	C III	0.19	0.925	0.21	5876	He I	11.4	1.384	8.2
4649, 50	O III, C III	0.44	0.926	0.48	6005	He II	0.11	1.436	0.08
4658	[Fe III]	0.24	0.927	0.26	6037	He II	0.14	1.447	0.10
4658	C III	0.15	0.927	0.16	6074	He II	0.18	1.461	0.12
4686	He II	56.4	0.938	60.1	6087	[Fe VII] [Ca V]	0.11	1.465	0.075
4711 4713	[Ar IV He I	7.92	0.944	8.4	6102	[K IV	0.25	1.471	0.17
4724, 26	[Ne IV]	1.23	0.95	1.29	6118	He II	0.19	1.480	0.13
4740	[Ar IV]	7.4	0.957	7.7	6133	[Fe III]	0.18	1.487	0.12
4861	Hβ	100	1.0	100	6170	He II	0.13	1.500	0.09
4922	He I	0.69	1.023	0.67	6233	He II	0.18	1.524	0.12
4931	[O III]	0.29	1.026	0.28	6300	[O I]	26.8	1.548	17.3
4944	[Fe VII]	0.18	1.032	0.17	6312	[S III]	2.42	1.552	1.56
4959	[O III]	512	1.027	499	6363	[O I]	8.2	1.570	5.2
4972	[Fe VI]	0.10	1.04	0.10	6406	He II	0.43	1.583	0.27
5007	[O III]	1570	1.063	1480	6435	[Ar V]	2.1	1.593	1.31
5015	He I	0.79	1.065	0.74	6548	[N II]	383	1.630	235
5041	Si II	0.089	1.067	0.083	6563	Hα	463	1.636	283
5048	He I	0.071	1.07	0.066	6584	[N II]	1190	1.641	727
6678	He I	4.0	1.673	2.4	7530	[Cl IV]	0.71	1.960	0.36
6717	[S II]	8.2	1.684	4.9	7593	He II	0.42	1.978	0.21
6730	[S II]	13.4	1.690	7.9	7726	[S I]	0.44	2.014	0.22
6780		.39	1.70	0.23	7751	[Ar III]	11.3	2.024	5.6
6810	He II	0.56	1.708	0.33	8046	[Cl IV]	1.70	2.097	0.8
7005	[Ar V]	6.1	1.786	3.4	8196		0.53	2.136	0.25
7065	He I	5.8	1.804	3.2	8236	He II	3.2	2.145	1.5
7135	[Ar III]	41.2	1.830	22.6	8437	P 18	0.77	2.198	0.35
7170	[Ar IV]	1.53	1.843	0.83	8467	P 17	0.82	2.206	0.37
7237	[Ar IV]	0.67	1.866	0.36	8502	P 16	1.04	2.216	0.47
7262	[Ar IV]	0.49	1.876	0.26	8545	P 15	1.36	2.226	0.61
7281	He I	0.70	1.883	0.37	8577	[Cl II]	1.95	2.238	0.87
7319, 30	[O II]	24.9	1.900	13.1	8578	P 14	1.52	2.238	0.68

[a]The intensities uncorrected for interstellar extinction.

[b]The extinction factor by which I_o is to be divided to obtain I_c.

[c]The intensities corrected for extinction.

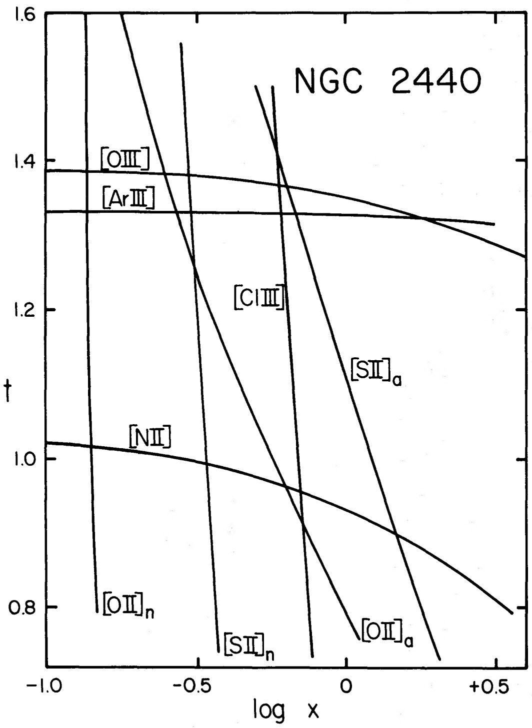

FIG. 1.—Constraints on electron density and temperature imposed various line ratios: [O II]$_n$ = $I(\lambda3729)/I(\lambda3726)$; [O II]$_a$ = $I(\lambda7325)/I(\lambda3727)$; [S II]$_n$ = $I(\lambda6731)/I(\lambda6717)$; [S II]$_a$ = $(\lambda4072)/I(\lambda6720)$; [N II] = $I(\lambda\lambda6548, 6584)/I(\lambda5755)$; [O III] = $I(\lambda\lambda5007, 4959)/I(\lambda4363)$; [Ar III] = $I(\lambda7135)/I(\lambda5192)$; [Cl III] = $I(\lambda5518)/(\lambda5538)$.

Our detection of O III] $\lambda1663$ allows a determination of the temperature in the O^{++} zone independent of the $\lambda4363$ intensity that is usually used in nebular studies. Adopting the value of Baluja, Burke, and Kingston (1980*a*) $\Omega(^3P, ^5S) = 1.22$ and of Eissner and Seaton (1974), $\Omega(^3P, ^1D) = 2.4$, we find

$$I(\lambda1663)/I(\lambda5007, 4959) = 1.53 \times 10^{-2.49/t}, \quad (1)$$

where $t = T/10^4$ K. For the intensities quoted in Tables 1 and 2, this gives $T = 13{,}700$ K, in agreement with the optical result.

The ratio [Ar IV] $\lambda4711/\lambda4740$ is potentially important because it samples the electron density in a zone of higher ionization than the other indicators. However, $\lambda4711$ is contaminated by other lines. From the observed intensities of He I $\lambda4471$ and $\lambda5876$ and the theoretical He II decrements (Brocklehurst 1972), we estimate that $I(\lambda4713) = 0.3$. A straightforward calculation using the published collision strengths and transition probabilities for [Ne IV] allows us to estimate $I(\lambda4714, 4716) = 0.8$ from the observed intensity of $\lambda\lambda4724, 4726$. The corrected line ratio, $I(\lambda4711)/I(\lambda4740) = 0.95$, corresponds to $\log x = 0.1$, where $x \equiv t^{-1/2}N_e/10^4$ cm^{-3}. This is somewhat higher than the value $\log x = -0.5$ indicated by [O II] and [S II], but it is still too low to affect the inferred [O III] temperature significantly. NGC 2440 does not give evidence of such high electron densities as the value 6×10^4 cm^{-3} found in the high-excitation PN NGC 7027 (Miller and Mathews 1972; Kaler *et al.* 1976).

Milne and Aller (1975) measured a 6 cm continuum flux $S = 0.40$ Jy from NGC 2440 which, for a distance $d = 1.35$ kpc (Cahn and Kaler 1971; Milne and Aller 1975), corresponds to a hydrogen recombination rate $Q(H^0) = 6 \times 10^{46}$ s^{-1} throughout the nebula. At the adopted density this corresponds to $\sim 10^{-1.0}\, M_\odot$ of ionized gas. The ionizing photon luminosity of the star $Q(H^0)$, may be greater if some of the ionizing photons escape. O'Dell (1963) gives $F(H\beta) = 10^{-10.56}$ ergs s^{-1} cm^{-2}, which, together with the radio flux, gives an extinction $c = 0.65$. The excellent agreement with the reddening indicated by the Balmer decrement indicates that most of the extinction is external to the emitting region. If we assume that most of the light comes from a core of radius $\sim 10''$, then the above $Q_n(H^0)$ corresponds to an rms electron density ~ 3000 cm^{-3}. Since this is close to the density inferred from the line ratios, we conclude that the nebular core has a fairly large filling factor, $f > 10^{-1}$.

Recently, Harlan and Miller (1979) reported the probable detection of the central star of NGC 7027, with a magnitude in the yellow of about 15. This nebula and NGC 2440 have similarly high ionization, and presumably they have central stars with similar temperatures. Therefore, we may predict on the basis of the relative radio fluxes from the two objects that the central star of NGC 2440 has $m \approx 18$.

IV. PHOTOIONIZATION MODELS

a) *Parameters*

We have computed several models of the ionization structure of NGC 2440 with the program described by Shields (1978*a*). This program includes the usual processes of photoionization, radiative and dielectronic recombination, and line and continuum emission; and charge transfer (Péquignot, Aldrovandi, and Stasinska 1978) is now included. Most of our results are based on a reference model, Model 1, computed with coefficients for various physical processes as given in the Appendix. In § VI, we briefly explore some other values for various charge transfer coefficients.

For the sake of tractability, we have limited the calculations to a simple model with spherical geometry, a single density, and a filling factor of unity. In order to given an [O II] $\lambda3729/\lambda3726$ line ratio in reasonable agreement with that observed, a value $N = 4000$ cm^{-3} for the atomic number density was adopted. (The O^+ zone has N_e somewhat lower than N.) The central star had an ionized photon luminosity $Q(H^0)$, $Q(H^0) = 6 \times 10^{46}$ s^{-1}, the minimum found in § III. We used a central star temperature $T_* = 166{,}000$ K, for which stellar atmosphere fluxes, based on the models of Hummer and Mihalas (1970*a*, *b*) were conveniently available. For our purposes, the resulting value of $I(\lambda4686)/I(H\beta) = 0.5$ is adequately close to that observed.

For the chemical abundances, we used the results of a preliminary analysis of NGC 2440 by Aller and Keyes (1980): $12 + \log N(A)/N(H) = (11.08, 8.52, 8.80, 8.72, 8.08, 6.98, 5.38, 6.44, 6.22, 4.58, 4.80)$ for (He, C, N, O, Ne, S, Cl, Ar, Na, K, Ca). For (Mg, Si, Fe) we used abundances (6.20, 6.25, 6.10) on the basis of the solar system abundances by Ross and Aller (1976) and the assumption that these elements all have the mean depletion -1.4 dex found for the gas-phase abundance of iron in planetary nebulae by Shields (1978*b*). Only the elements with log abundances greater than 7.0 significantly affect the thermal equilibrium.

The Strömgren sphere radius $[N(H^+)/N(H^0) = 1]$ in Model 1 occurs at $R = 1.6 \times 10^{17}$ cm, in reasonable agreement with the observed radius of the bright core. The corresponding value of the ionization parameter, $U \equiv Q(H^0)/4\pi R^2 N c$, is 1.6×10^{-3}. This parameter determines the fractional abundances of the "transition zone" ions such as N^+, O^+, etc. Model 1 gives $N(O^+)/N(O^{++}) = 0.5$, in reasonable agreement with the "observed" value described in § V. This indicates that the model has U acceptably close to the mean value characterizing the actual nebula, and the model therefore should give a valid estimate of the fractional abundances of most ions as long as the relevant atomic data are accurate.

b) *Results*

Our philosophy is not to attempt to fine-tune the models to fit the observations but rather to extract from the approximate model some interesting physical quantities that can be compared with ionic abundances and temperatures derived from the observed line ratios. Thus, we given in Table 3 a list of ionization fractions,

$$\langle X(A^{+i})\rangle \equiv \frac{\int X(A^{+i}) N_e dV}{\int N_e dV}, \tag{2}$$

TABLE 3

Temperature and Ionization in Model 1

Element	Ion[a] I	II	III	IV	V	VI	VII
H	1.27(-1) 0.86	8.7(-1) 1.39					
He	7.4(-2) 0.72	5.3(-1) 1.20	3.9(-1) 1.59				
C	1.2(-3) 0.98	1.7(-1) 0.90	3.9(-1) 1.23	2.7(-1) 1.50	1.7(-1) 1.69		
N	5.9(-2) 0.75	2.4(-1) 1.04	3.1(-1) 1.30	1.6(-1) 1.50	1.6(-1) 1.63	6.4(-2) 1.76	
O	1.2(-1) 0.83	1.6(-1) 1.08	3.2(-1) 1.28	1.5(-1) 1.49	6.2(-2) 1.60	1.8(-1) 1.68	1.6(-2) 1.82
Ne	2.0(-2) 0.65	5.4(-2) 0.84	3.8(-1) 1.14	2.4(-1) 1.40	2.2(-1) 1.58	7.6(-2) 1.71	6.3(-3) 1.89
Na	3.2(-4) 0.80	7.9(-2) 0.80	3.0(-1) 1.12	2.2(-1) 1.34	2.6(-1) 1.53	1.2(-1) 1.66	1.3(-2) 1.84
Mg	5.6(-3) 1.00	4.1(-1) 1.08	2.4(-1) 1.34	1.2(-1) 1.53	9.5(-2) 1.61	1.1(-1) 1.70	1.4(-2) 1.85
Si	4.9(-4) 0.90	1.0(-1) 0.81	7.9(-2) 1.07	3.2(-1) 1.28	4.4(-1) 1.48	5.6(-2) 1.69	2.1(-3) 1.92
S	3.2(-4) 0.95	1.3(-1) 0.84	2.2(-1) 1.12	2.3(-1) 1.36	2.6(-1) 1.48	1.6(-1) 1.69	
Cl	2.0(-2) 0.85	9.8(-2) 0.83	1.3(-1) 1.15	4.9(-1) 1.32	1.5(-1) 1.58	6.0(-2) 1.68	4.7(-2) 1.77
Ar	5.0(-2) 0.71	2.91(-2) 0.83	1.1(-1) 1.09	5.6(-1) 1.30	9.6(-2) 1.58	9.4(-2) 1.68	5.4(-2) 1.79
K	8.8(-5) 0.73	7.4(-2) 0.75	5.9(-2) 1.02	3.8(-1) 1.19	1.8(-1) 1.43	1.6(-1) 1.57	1.1(-1) 1.66
Ca		4.0(-3) 0.85	1.6(-1) 1.05	3.6(-1) 1.20	1.7(-1) 1.41	2.0(-1) 1.56	1.1(-1) 1.66
Fe	2.9(-4) 0.92	1.2(-1) 0.82	7.7(-2) 1.09	4.3(-1) 1.25	1.4(-1) 1.50	1.3(-1) 1.62	7.4(-2) 1.69

[a] $\langle X(A^{+i})\rangle$, $\langle t(A^{+i})\rangle$.

where $X(A^{+i}) \equiv N(A^{+i})/N(A)$ for any element A, and ion-weighted temperatures,

$$\langle t(A^{+i})\rangle \equiv \frac{\int t(A^{+i})X(A^{+i})N_e dV}{\int X(A^{+i})N_e dV} . \qquad (3)$$

This approach should give the reader a feeling for the role the model plays and for the uncertainties involved. Also, the model results presented in this form may be more useful for application to other high-excitation planetary nebulae. For example, the ionization fractions of the transition zone ions should vary together for moderate changes in U; the ionization fractions of most He^{++} zone ions should vary roughly as $\langle X(He^{++})\rangle$; and the temperature differentials, $\langle t(A^{+i})\rangle - \langle t(B^{+j})\rangle$, should change relatively little for moderate changes in model parameters.

c) *The T* (O III) *Problem*

By and large, the model gives ionic abundance ratios in reasonable agreement with those observed (see § V). However, a significant discrepancy arises with the [N II] and [O III] temperatures. Model 1 gives $\langle t(N^+)\rangle = 1.04$ and $\langle t(O^{++})\rangle = 1.28$, whereas we observed t(N II) = 1.01 and t(O III) = 1.38. The observed O III temperature is considerably higher than predicted, and the differential $\Delta t \equiv t$(O III) − t(N II) is significantly larger than predicted.

An obvious way to raise t(O III) is to lower the abundances. However, changes in the overall heavy-element abundances in trial models, within limits consistent with the "observed" ionic abundances (§ V), were ineffective, particularly in altering Δt.

Is something altering the [O III] λ4363/λ5007 line ratio? The problem probably is not due to stratification in the nebula, since Torres-Peimbert and Peimbert (1977) found t(N II) = 9500 K and t(O III) = 13,400 K from photoelectric scans of the entire bright core of the nebula. The agreement between the temperatures indicated by λ4363 and λ1663 also supports the reliability of our [O III] temperature. The electron densities derived in § III are too low to produce significant deactivation of λ5007; the density derived from [Ar IV] is especially important since these lines are emitted from roughly the same zone as are the [O III] lines. Inspection of the [O III] intensities of several high-excitation planetary nebulae in Kaler's (1976) catalog indicates more variation in λ4363 than in λ5007, so that, if anything, I(λ4363) is suspect. Continuum fluorescence must be insignificant since any UV resonance line could absorb at most a fractional width $\Delta v/c \approx 10^{-4.5}$ of the stellar continuum. Line fluorescence in O III has been discussed by Burgess (1967) and Shull and McCray (1978), but it appears to be negligible in nebulae.

Could some of the [O III] emitting gas be heated by a process other than photoionization? Kwok, Purton, and FitzGerald (1978) have emphasize the dynamical importance of fast ($\sim 10^3$ km s^{-1}) wind from the central star of a PN. Such a wind might have a mass flux $\dot{M} \sim 10^{-6}\ M_\odot$ yr^{-1}. Models by Cox (1972) suggest that shocked gas with cosmic abundances emits about 0.2 eV per H atom in λ4363 as it passes through the O^{++} stage during its cooling and recombination. We might therefore expect $\sim 10^{31}$ ergs s^{-1} in λ4363 from the fast wind (if it succeeds in cooling in the available time), an insignificant amount compared with the observed luminosity of $10^{33.9}$ ergs s^{-1} in λ4363.

We are unable to explain the large difference between the [N II] and [O III] temperatures observed in NGC 2440.

V. THE CHEMICAL ABUNDANCES

We first derive ionic abundances from the line intensities using standard procedures and a minimum of reliance on the model. Then we shall derive elemental abundances with the aid of ionization corrections derived from Model 1.

a) *Ionic Abundances*

The electron density in NGC 2440 is sufficiently low that nearly all ionic abundances can be derived from observed line intensities that are not subject to collisional deactivation. The main physical variable required is the temperature characteristic of the zone where a particular line is emitted. In order to maintain maximum contact with the observed temperatures, we have adopted three temperature zones: (1) an O^+ zone with $t = 1.00$ as given by the [N II] line ratio; (2) an O^{++} zone with $t = 1.38$; and (3) an He^{++} zone with $t = 1.55$, an average of the Model 1 temperatures for the observed ions that reside in this zone. It is also useful to have mean temperatues for the He^+ zone and the entire H^+ zone. These we have constructed by assuming that O^+ and O^{++} fill the He^+ zone, and weighting the temperatures of the O^+, O^{++}, and He^{++} zones according to the O^+/O^{++} and He^+/He^{++} measured abundance ratios. Table 4 gives for each zone its mean temperature and its fraction of the total nebular emission measure ($\int N_e^2 dV$).

The ionic abundances are given by the formula

$$\frac{N(A^{+i})}{N(H^+)} = \frac{E_{4,2}{}^0}{E^0}\frac{I(\lambda)}{I(H\beta)}, \qquad (4)$$

where $E_\lambda{}^0 = E_\lambda/10^{-25}$ ergs cm^3 s^{-1} and E_λ is the emissivity per ion per unit electron density. For Hβ, we have from Brocklehurst(1971) $E_{4,2}{}^0 = 1.24t^{-0.87} = 0.92$, where we have used $\langle t(H^+)\rangle = 1.41$ from Table 4. For

TABLE 4

TEMPERATURE ZONES FOR IONIC ABUNDANCES

Zone	$\langle t\rangle$	Fraction of Emission Measure
O^+	1.00	0.16
O^{+2}	1.38	0.34
He^+	1.27	0.50
He^{+2}	1.55	0.50
H^+	1.41	1.00

most of the collisionally excited lines, the reciprocal emissivity is adequately given by

$$(E_{\lambda}{}^{0})^{-1} = A \times 10^{b/t} t^{1/2} , \tag{5a}$$

where

$$A = 5.8 \times 10^{-7} (\omega/\Omega) \lambda_{\mu} B^{-1} \tag{5b}$$

and

$$b = 0.503 \chi_{eV}/t . \tag{5c}$$

Here ω is the statistical weight of the level from which excitation occurs, Ω is the relevant collision strength, λ_{μ} is the wavelength in microns, B is the branching ratio, and χ_{eV} is the excitation potential in electron volts. (If the excitation is between the same levels as the observed line then $0.503\chi_{eV} = 0.625/\lambda_{\mu}$.)

Table 5 gives the ionic abundances derived in this fashion. Included in the table are the coefficients for calculating the emissivity according to equations (5a, b, c) based on the collision strengths listed in the Appendix. Also given is the mean temperature adopted for each ion. Most ions were assigned to either the O^+, O^{++}, or He^{++} zone; but for a few ions that straddled two zones in the model, we adopted an intermediate temperature. For O^+, S^+, and Ne^+, the emissivity was derived from five-level population computations. The special cases of helium, carbon, and iron are discussed below.

b) Elemental Abundances

The total abundance of an element is given by

$$\frac{N(A)}{N(\mathrm{H})} = \frac{N(A^{+i})}{N(\mathrm{H}^+)} \frac{\langle X(\mathrm{H}^+) \rangle}{\langle X(A^{+i}) \rangle} , \tag{6}$$

where A^{+i} refers to one or more observed stages of ionization. Table 6 gives, for each element, the ionization stages included in the abundance determination, the combined ionization function for these ions, and the elemental abundance. The ionization fractions generally were taken from Model 1 in a straightforward manner. However, for the ions in the He^{++} zone, the fractional abundance was increased by a factor ~ 1.3 equal to

TABLE 5

ABUNDANCES OF IONS

Ion	λ	Transition	A	b	$\langle t \rangle$	$\frac{I(\lambda)}{I(\mathrm{H}\beta)}$	$\frac{N(A^{+i})}{N(H^+)}$
C II]	2326	^2P–^2D	2.6 (−7)	2.71	1.00	0.69	8.0 (−5)
C III]	1906, 1909	^1S–^3P	7.7 (−8)	3.28	1.38	7.5	1.5 (−4)
C IV	1548, 1550	^2S–^2P	2.1 (−8)	4.03	1.38	4.5	8.5 (−5)
[N II]	6584, 6548	^3P–^1D	1.29(−6)	0.95	1.00	9.6	1.02(−4)
N III]	1747–1754	^2P–^4P	3.2 (−7)	3.57	1.38	1.40	1.9 (−4)
N IV]	1487	^1S–^3P	1.06(−7)	4.20	1.38	1.98	2.5 (−4)
N V	1239, 1241	^2S–^2P	2.2 (−8)	5.04	1.55	1.13	5.1 (−5)
[O II]	7320, 7330	^2D–^2P	…	…	1.00	0.131	8.6 (−5)
[O III]	5007, 4959	^3P–^1D	1.10(−6)	1.26	1.38	19.8	1.9 (−4)
O IV]	1403, 1409	^2P–^4P	3.6 (−7)	4.45	1.55	0.50	1.5 (−4)
O V]	1371	^1S–^3P	1.55(−7)	4.60	1.55	<0.13:	<2.1 (−5):
[Ne III]	3868, 3968	^3P–^1D	1.53(−6)	1.60	1.38	1.56	3.7 (−5)
[Ne IV]	2438, 2444	^4S–^2D	4.2 (−7)	2.58	1.55	1.31	3.0 (−5)
[Ne IV]	4714–4726	^2D–^2P	6.3 (−6)	3.88	1.55	2.1 (−2)	4.8 (−5)
[Ne V]	3426, 3346	^3P–^1D	8.6 (−7)	1.84	1.55	1.28	1.9 (−5)
[Na IV]	3241, 3362	^3P–^1D	1.5 (−6)	1.89	1.38	1.8 (−2)	6.8 (−7)
Mg II	2800	^2S–^2P	1.8 (−8)	2.23	1.20	0.04:	5.3 (−8)
[Mg V]	2783, 2928	^3P–^1D	1.51(−6)	2.27	1.55	0.09:	4.5 (−6)
Si III]	1892	^1S–^3P	2.2 (−8)	3.30	1.00	0.07:	2.8 (−6):
Si IV	1391	^2S–^2P	9.6 (−9)	4.49	1.38	<0.2	<3.0 (−6)
[S II]	4068, 4076	^4S–^2P	…	…	1.00	4.4 (−2)	5.9 (−7)
[S III]	6312	^1D–^1S	3.4 (−6)	1.66	1.00	1.6 (−2)	2.2 (−6)
[Cl II]	8577, 9126	^3P–^1D	9.4 (−7)	0.71	1.00	8.7 (−3)	3.8 (−8)
[Cl III]	5518, 5538	^4S–^2D	3.3 (−7)	1.13	1.00	6.3 (−3)	2.6 (−8)
[Cl IV]	7530, 8046	^3P–^1D	1.7 (−6)	0.81	1.38	1.2 (−2)	8.3 (−8)
[Ar III]	7135, 7751	^3P–^1D	7.5 (−7)	0.88	1.00	0.28	1.4 (−6)
[Ar IV]	7170, 7262	^2D–^2P	6.2 (−6)	2.18	1.38	1.5 (−2)	3.8 (−6)
[Ar IV]	4711, 4716	^4S–^2D	6.9 (−7)	1.32	1.38	0.15	1.0 (−6)
[Ar V]	6435, 7005	^3P–^1D	2.7 (−6)	0.92	1.55	1.31(−2)	1.6 (−7)
[K IV]	6102, 6796	^3P–^1D	1.6 (−6)	0.99	1.38	2.1 (−3)	1.8 (−8)
[Ca V]	5309, 6087	^3P–^1D	2.6 (−6)	1.14	1.55	1.0 (−3)	1.6 (−8)
[Fe V]	4227	$^5D_4$–$^3H_4$	2.9 (−6)	1.49	1.55	2.8 (−3)	8.7 (−8)
[Fe IV]	5146	$^4F_{7/2}$–$G_{7/2}$	4.0 (−6)	1.36	1.55	0.9 (−3)	3.2 (−8)
	4973	$^4F_{9/2}$–$G_{7/2}$	4.1 (−6)	1.36	1.55	1.0 (−3)	3.6 (−8)
	5176	$^4F_{9/2}$–$G_{9/2}$	3.8 (−6)	1.56	1.55	1.2 (−3)	5.4 (−8)
[Fe VII]	6087	$^3F_3$–$^1D_2$	4.8 (−6)	1.15	1.55	5.9 (−4)	1.8 (−8)
	5159	$^3F_3$–$^3P_1$	1.5 (−5)	1.29	1.55	1.1 (−3)	1.3 (−7)
	4944	$^3F_3$–$^3P_2$	1.7 (−5)	1.32	1.55	1.7 (−3)	2.4 (−7)

TABLE 6

ELEMENTAL ABUNDANCES[a]

			12 + log N				
			NGC 2440				
ELEMENT	IONS	⟨X⟩	Model 1	Interpolation	Non-Plankian	PN	Solar System
H	+1	0.93	12.00	12.00	12.00	12.00	12.00
He	+1, 2	0.87	11.04 ± 0.05	11.07	11.07	11.02	11.00
C	+1, 2, 3	0.83	8.58 ± 0.15	8.37	8.52	9.10:	8.65
N	+1, 2, 3, 4	0.87	8.83 ± 0.15	8.79	8.88	7.97	7.96
O	+1, 2, 3	0.61	8.83 ± 0.15	8.61	8.55	8.66	8.87
Ne	+2, 3, 4	0.85	8.01 ± 0.10	8.03	8.02	8.02	8.05
Na	+3	0.22	6.4 ± 0.4	6.4	6.3	6.23	6.30
Mg	+1	0.41	5.2 ± 0.5	...	...	...	7.60
Si	+3	0.25	<7.1:	...	...	...	7.65
S	+1, 2	0.35	6.8 ± 0.3	6.4	7.0:	7.10	7.23
Cl	+1, 2, 3	0.72	5.2 ± 0.3	5.3	5.4	5.26	5.5
Ar	+2, 3, 4	0.77	6.7 ± 0.4	6.5	6.4	6.38	6.57
K	+3	0.38	4.6 ± 0.4	4.6	4.8	4.90	5.14
Ca	+4	0.22	4.8 ± 0.4	4.9	5.0	5.10	6.31
Fe	+4, 5, 6	0.44	5.7 ± 0.4	...	...	...	7.58

[a] Ions and their combined ionization fractions are based on Model 1 as described in the text. The resulting abundances are compared with the UCLA results for interpolated ionization corrections and for model fitting with a non-Planckian ionizing continuum. The PN average abundances are from Aller 1978 except for sulfur, for which results by Dinerstein 1980*a*, *b* have been used. The solar system values are from Aller 1980.

the ratio of the observed He^{++} fraction to that in the model.

Helium.—Helium is a special case in that the He I and He II lines are formed by radiative recombination. We used the effective recombination coefficients of Brocklehurst (1971, 1972) for He I and He II, respectively. Taking into account the line intensities, we assigned relative weights of (1, 2, 1) for He I λλ4471, 5876, 6678 and (1, 3, 1) for He II λλ4541, 4686, 5411. A feature at λ2838 with $I = 0.07I(H\beta)$ is much stronger than the expected intensity of He I λ2830.

Torres-Peimbert and Peimbert (1977) find He/H = 0.15, larger than our value He/H = 0.11; the difference results from larger measured He I line intensities in their study.

Carbon.—Table 6 gives a carbon abundance based entirely on the collisionally excited lines in the UV. However, several permitted lines are observed in the optical that may result from recombination. Using the effective recombination coefficients quoted by Seaton (1978), we find from C II λ4267 a value $C^{+2}/H^{+} \sim 4 \times 10^{-4}$, rather larger than the value 1.5×10^{-4} derived from C III λ1909. From the C III λ4650 multiplet, allowing for dielectronic recombination following Torres-Peimbert and Peimbert (1977), we find $C^{+3}/H^{+} \sim 7 \times 10^{-5}$. The last two values are roughly consistent with the C^{+3} abundance derived from λ1549 and the C^{+2}/C^{+3} ratio in Model 1. Torres-Peimbert and Peimbert (1977) derive $12 + \log N(C)/N(H) = 9.0$ for NGC 2440 from the optical "recombination" lines, consistent with the preceding remarks. Because the ultraviolet lines give reasonable abundances for the ions of O and N, we tentatively adopt the ultraviolet values for the carbon abundance.

Magnesium.—The derived Mg^{+4}/Mg^{+} ratio is two orders of magnitude larger than predicted by the models. This resembles the result of Péquignot and Stasinska (1980) for NGC 7027. They propose that magnesium is locked up in grains in the outer part of the nebula (Mg^{+}) but not in the inner part (Mg^{+4}). Our results are consistent with this idea, given that the identification of λ2783 with [Mg V] is correct. The derived abundance of Mg^{+4} in NGC 2440, together with its ionization fraction from Model 1, implies [Mg/H] ≈ 0.0; but the analogous calculation for Mg^{+} (Table 6) gives [Mg/H] ≈ −2.

Silicon.—Si III] and Si IV give discrepant abundances. From the profile of the feature at λ1400, we estimate $I < 20$ for Si IV λ1391. This leads to a Si^{+2}/Si^{+3} ratio considerably larger than predicted by our models. In view of the difficulty of measuring the weak Si III] feature on the instrumental wing of C III], we give in Table 6 a provisional limit on the silicon abundance based on Si IV alone. (However, Harrington and Marionni 1980 find a Si III] intensity in NGC 2440 that is similar to our result.)

Sulfur.—The ionization structure of sulfur in nebulae is controversial (see Dinerstein 1980*a*, *b* and references therein). Model 1 gives a S^{+2}/S^{+3} ratio close to those observed by Dinerstein (1980*b*) for nebulae with O^{+}/O^{++} ratio similar to that in NGC 2440. This model includes $S^{+3} + H^{0}$ charge transfer at a rate coefficient estimated empirically by Péquignot, Aldrovandi, and Stasinska (1978). In § VI a model is described which includes rate coefficients for $S^{+3} + H^{0}$ and $S^{+4} + H^{0}$ calculated by Butler and Dalgarno (1980). These reactions increase $\langle X(S^{+1,2})\rangle$ by less than 0.1 dex from the value in Model 1.

Iron.—The forbidden line emissivities have been tabulated for [Fe VII], [Fe VI], and [Fe V] by Nussbaumer and Osterbrock (1970), Nussbaumer and Storey (1978), and Garstang, Robb, and Rountree (1978), respectively. From these numerical values, we have derived the constants listed in Table 5 for use in equations (5a, b, c). Assigning equal weights to the various lines of [Fe VII] and [Fe VI], we find average abundances $Fe^{+}/H^{+} = 1.3 \times 10^{-7}$ and $Fe^{+6}/H^{+} = 4.1 \times 10^{-8}$. These values were used in arriving at the entries for iron in Table 6.

c) Uncertainties

The uncertainties are dominated by various possible systematic errors. In Table 6, we give our guess as to the maximum likely error in the derived abundances of the elements in NGC 2440. These are based on consideration of (1) the effect of raising or lowering the electron temperature by ~ 1000 K, (2) the magnitude of the ionization correction, (3) the line intensities, (4) the possible uncertainty in the collision strengths, and (5) the consistency between ionic abundances derived from different lines. In most cases, the ratios of the abundances of elements heavier than helium have smaller uncertainties because of partial cancellation of the effects of temperature errors.

d) Discussion

Table 6 compares the abundances in NGC 2440 with the solar system values (Aller 1980) and with an averaged compilation for other planetary nebulae (Aller 1978). For oxygen and most heavier elements, the abundances are similar to the solar system and PN values, consistent with a Population I progenitor for NGC 2440.

Iron shows the usual strong depletion that presumably results from its involvement in grains (Shields 1978*b*). A similarly strong depletion is shared by the refractory elements calcium and magnesium. The calcium depletion is similar to that in other planetary nebulae. Silicon shows a depletion of at least ~ 0.5 dex, based on an estimate of the maximum contribution of Si IV to the blend at $\lambda 1400$.

The pattern for all the refractory elements appears to be depletion by about 1.5–2.0 dex, consistent with the idea that the gas-phase abundances of refractory elements result from a small contribution to the nebular mass by a hot wind from the central star (Shields 1980). The lack of depletion of the heavy elements sulfur, chlorine, and argon supports the idea that the depletions of magnesium, silicon, calcium, and iron result from grain formation. On the other hand, Morris *et al.* (1979) give evidence that the wind emanating from IRC 10216 may have about 1% of its silicon involved in the molecules SiO and SiS. This raises the possibility that the gas-phase refractory atoms in planetary nebulae are those that formed molecules rather than grains during the ejection phase; the molecules were later dissociated whereas the grains remain.

The remarkably high nitrogen abundance in NGC 2440 has been noted by previous authors (e.g., Aller 1967; Peimbert and Torres-Peimbert 1977). Our results, giving [N/H] = +0.8, should be more accurate because the UV observations allow us to measure $N^{+2,3,4}$ in addition to the usual optical determination of the N^{+} abundance. This huge amount of nitrogen must come from the processing of carbon manufactured by the progenitor itself, since oxygen is undepleted and the excess nitrogen exceeds the cosmic abundance of carbon. Assuming that the UV value for the nebular carbon abundance is accurate, the object would have a carbon abundance [C/H] = +0.4 (C/O ~ 1) if the excess nitrogen had remained mostly in the form of carbon. For NGC 7662, in fact, Bohlin, Harrington, and Stecker (1978) find C/O ~ 1 and [N/O] $\approx +0.1$. This suggests that the extreme nitrogen excess in NGC 2440 and the lower carbon abundance may result from more efficient processing of carbon into nitrogen in the progenitor; the amount of fresh carbon originally injected into the envelope could have been "normal" for a high-excitation PN.

Surface abundances in intermediate mass stars after the "third dredge-up" phase have been discussed by Becker and Iben (1980) and Renzini and Voli (1980). The models by Becker and Iben approach the nitrogen enrichment of NGC 2440 only for progenitor masses $\sim 8\ M_{\odot}$, and these have carbon and helium abundances much larger than observed. One may speculate that some mixing process such as meridional circulation (Sweigart and Mengel 1979) has facilitated $^{12}C \rightarrow {}^{14}N$ conversion in the envelope following carbon enrichment. The required preconversion carbon abundance occurs in Becker and Iben's (1980) models for a progenitor of $\sim 2\ M_{\odot}$, which would give a helium abundance consistent with our determination for NGC 2440. Alternatively, Scalo, Despain, and Ulrich (1975) discuss the possibility of CNO processing at the base of the convective envelope during the double shell-burning phase in stars down to $1.5\ M_{\odot}$. Calculations of this process by Renzini and Voli (1980) give N/O values like that in NGC 2440 for progenitor masses as low as $3.4\ M_{\odot}$, but the calculated C/O value is too large.

Becker and Iben note that wholesale conversion of ^{12}C to ^{14}N in all low- and intermediate-mass stars would have supplied the interstellar gas with much more ^{13}C than observed. However, the high nitrogen abundance in NGC 2440 is exceptional.

Infrared observations of planetary nebulae generally show features suggestive of SiC and not the silicate features seen in the spectra of dust shells around O-rich stars (Aitken *et al.* 1979). This is consistent with indications that most planetary nebulae have C/O > 1, so that CO molecules incorporate all the oxygen before silicates can form. Since NGC 2440 appears to have C/O < 1, it may be a candidate to show silicate features. On the other hand, some carbon may be hiding in grains (Mathis 1978).

By way of comparison, a somewhat different model was obtained with a computer program (Keyes and Aller 1978) modified from that by Balick (1975). The program included the charge transfer coefficients by Butler, Heil, and Dalgarno (1980) and Butler and Dalgarno (1980), for

TABLE 7

COMPARISON OF CHARGE-TRANSFER AND RADIATIVE RECOMBINATION RATES[a]

Ion reacting with H^0	log k ($cm^3\ s^{-1}$)	log $(kN_{H^0}/\alpha N_e)$
C^{+2}	−12.00	−0.9
C^{+3}	−8.44	+1.0
C^{+4}	−9.1	−0.7
N^{+2}	−9.07	+1.3
N^{+3}	−8.54	+0.7
N^{+4}	−9.8	−1.3
O^{+2}	−9.11	+1.6
O^{+3}	−8.07	+1.0
O^{+4}	−9.6	−1.3
Ne^{+2}	−14.5	−1.9
Ne^{+3}	−8.24	+1.3
Ne^{+4}	−8.2	−0.1
Mg^{+2}	−13.1	−2.7
Mg^{+3}	−8.2	+1.2
Mg^{+4}	−8.2	+0.2
Si^{+3}	−9.4	+0.9
Si^{+4}	−8.6	+0.9
S^{+2}	−14.0	−2.3
S^{+3}	−8.6	+1.4
S^{+4}	−8.2	+1.0
Ar^{+2}	−14.0	−1.8
Ar^{+3}	−8.4	+2.3
Ar^{+4}	−8.2	+0.3

[a] Charge-transfer rate coefficients $k(10^4\ K)$ for the process $A^{+i} + H^0 \rightarrow A^{+i-1} + H^+$ from quantal calculations by Butler, Heil, and Dalgarno 1980 for $C^{+2,3}$, $N^{+2,3}$, $O^{+2,3}$ and $Ne^{+2,3}$, and from Landau-Zener estimates by Butler and Dalgarno 1980 for the remaining ions. The comparison of charge-transfer and radiative recombination rates was made using recombination coefficients $\alpha(T)$ from Aldrovandi and Péquignot 1973. For each ion, N_{H^0}/N_e was evaluated at the radius in Model 1 where $N(A^{+i})/N(A^{+i-1}) = 1$.

which see Table 7. (Several reactions involving He^0 were included; but except for $Ar^{+2} + He^0$ they are important only for helium abundances several times solar, as noted by Butler and Dalgarno.) A material-bounded nebula of constant density was assumed, and the energy distribution of the central star was modified in an effort to reproduce such intensity ratios as [O II]/[O III], He II/He I, and [Ne V]/[Ne III]. For the adopted model, one then can estimate abundances from (1) values required in the model to reproduce observed intensities or (2) an "interpolation" procedure involving ionization correction factors derived from the model in a manner like that described above for Model 1. The abundances obtained by means of these procedures are shown in Table 6. For most elements, the different procedures give abundances that agree to within about 0.1 dex; but larger discrepancies occur for some elements, presumably illustrating the component of uncertainty that enters from the modeling procedure. Errors in atomic cross-sections common to both programs, of course, will not show up in this comparison.

In § IVa we described our preference for the "interpolation" procedure over detailed fitting of line intensities. However, as an illustration of the success of the models, we note that in the "non-Planckian" model of Table 6 the ratios of predicted to observed intensities were (1.04, 0.97, 0.97, 1.56, 1.10, 1.04, 1.00, 1.12, 0.88, 0.80) for ($\lambda\lambda$5876, 4686, 6583, 5755, 3727, 5007, 4363, 3868, 3426, 6720) respectively. The agreement is good, except that this model, like Model 1, predicts a higher value of t(N II), relative to t(O III), then we have observed.

VI. CHARGE TRANSFER AND DIELECTRONIC RECOMBINATION

The importance of the $O^+ + H^0 \rightarrow 0^0 + H^+$ charge-transfer reaction in planetary nebulae has long been appreciated (Field and Steigman 1971; Williams 1973). More recently, it has become apparent that a variety of ions undergo important reactions with H^0. In particular, charge transfer may solve the problem of insufficient O^+ abundances in photoionization models (Préquignot, Aldrovandi, and Stasinka 1978).

When the analysis based on Model 1 was essentially completed, we received preprints by Butler, Heil, and Dalgarno (1980) and Butler and Dalgarno (1980) containing new charge transfer rate coefficients for a variety of reactions. The importance of these reactions is illustrated in Table 7. Here we give the ratio of the charge transfer recombination rate, $k(T)N(H^0)$, to the radiative recombination rate, $\alpha(T)N_e$, evaluated in Model 1 at the radius where the heavy ions connected by the reaction have equal abundances. When this ratio exceeds unity, charge transfer substantially alters the boundaries of the ionization zones and thus the ionization fractions. Evidently, many of the reactions are important at the quoted rates.

In order to explore further the importance of these reactions, we have computed Model 2, which is identical to Model 1 except that it includes all reactions for which Table 7 gives $k(N(H^0)/\alpha N_e > 10^{-1}$. The rates override those used in Model 1 for the ions involved; for other ions, we used the same rates as in Model 1. In addition, Model 2 includes a rate coefficient $k(10^4\ K) = 2 \times 10^{-9}$ cm^{-3} for the $Si^{+2} + H^0$ reaction (McCarroll and Valiron 1976). For comparison, Model 3 was computed without any charge transfer reactions. Table 8 gives the ionization fractions in Models 2 and 3 for those elements undergoing charge transfer.

For the lower ionization stages, the adopted charge transfer rates generally improve the agreement with observation, as revealed by a comparison of Tables 5 and 8. In particular, Model 3 suffers the familiar problem of giving too little O^+. [In Model 1, $\langle X(O^+)\rangle$ varies as $k(O^{++})^{0.35}$.] The observations also confirm the importance of the reactions of C^{+3}, N^{+2}, Ar^{+3}, and Ar^{+4} with H^0. If we assume a solar C/O ratio, then the observed S^{+2} abundance implies $\langle X(S^{+2})\rangle \approx 0.14$, which in turn implies the importance of the $S^{+3} + H^0$ charge transfer reaction. The latter reaction may explain the behavior of S^{+2} in planetary nebulae and H II regions (Pagel 1978; Barker 1978; Dinerstein 1980a, b). The reactios of N^{+3},

TABLE 8

EFFECT OF CHARGE TRANSFER ON IONIZATION FRACTIONS

Element	Ion[a] I	II	III	IV	V	VI	VII
C	1.2(-3)	1.8(-1)	4.8(-1)	2.0(-1)	1.4(-1)		
	1.0(-3)	1.4(-1)	2.3(-1)	4.5(-1)	1.7(-1)		
N	6.1(-2)	2.6(-1)	2.9(-1)	1.6(-1)	1.6(-1)	6.5(-2)	
	5.1(-2)	6.0(-2)	2.2(-2)	4.2(-1)	1.9(-1)	6.4(-2)	
O	1.2(-1)	1.8(-1)	4.4(-1)	5.5(-2)	4.1(-2)	1.5(-1)	1.5(-2)
	3.7(-2)	6.2(-2)	5.1(-1)	5.9(-2)	5.9(-2)	1.7(-1)	1.5(-2)
Ne	2.1(-2)	6.0(-2)	6.1(-1)	1.4(-1)	1.0(-1)	5.7(-2)	5.9(-3)
	2.0(-2)	5.3(-2)	4.1(-1)	2.3(-1)	2.1(-1)	7.3(-2)	5.9(-3)
Mg	5.9(-3)	4.4(-1)	3.0(-1)	1.2(-1)	4.4(-2)	7.3(-2)	1.3(-2)
	4.7(-3)	4.3(-1)	2.4(-1)	1.2(-1)	9.1(-2)	1.0(-1)	1.4(-2)
Si	3.9(-3)	4.1(-1)	6.8(-2)	2.5(-1)	2.4(-1)	4.5(-2)	2.0(-3)
	6.9(-4)	9.9(-2)	8.1(-2)	3.2(-1)	4.4(-1)	5.3(-2)	2.0(-3)
S	3.2(-4)	1.3(-1)	2.9(-1)	3.7(-1)	9.2(-2)	1.2(-1)	
	1.8(-4)	9.5(-2)	5.2(-2)	3.9(-1)	3.1(-1)	1.5(-1)	
Ar	5.1(-2)	3.5(-2)	4.5(-1)	3.0(-1)	4.3(-2)	6.6(-2)	4.8(-2)
	4.7(-2)	2.7(-2)	1.1(-1)	1.1(-1)	5.8(-1)	9.2(-2)	8.9(-2)

[a] $\langle X(A^{+i})\rangle$ for Models 2 and 3, respectively. Model 2 includes all important reactions listed in Table 7, whereas Model 3 omits all charge transfer.

O^{+3}, and Ne^{+4} with H^0 may proceed less rapidly than estimated by Butler and Dalgarno (1980) from the Landau-Zener approximation. These authors pointed out that some rates for high ionization stages might overestimated.

Nebular abundance analyses have often assumed that $N/O = N^+/O^+$, that is, $\langle X(N^+)\rangle/\langle X(O^+)\rangle = 1.0$. Model 2 has similar rates for the reactions of N^+ and O^+ with H^0, and it gives $\langle X(N^+)\rangle/\langle X(O^+)\rangle = 1.4$.

Although we did not include charge transfer with He^0 in models 1 or 2, we estimate for $Ar^{+2} + He^0$ that $kN(He^0)/\alpha N_e \approx 10$ at the Ar^+/Ar^{+2} boundary. From the behavior of analogous ions of other elements, it seems likely that this reaction will reduce $\langle X(Ar^{+2})\rangle$ by a factor of 2 or so. Unfortunately, the observed Ar^{+2}/Ar^{+3} ratio is too uncertain to provide a reliable test.

Since Models 1–3 give a Cl^+/Cl^{+2} ratio smaller than that observed, we experimented with various hypothetical values for the rate coefficient for $Cl^{+2} + H^0 \rightarrow Cl^+ + H^+$. Agreement with observation is achieved in Model 1 for $\log k \approx -10.0 \pm 0.5$. We also find $\log k(Cl^{+3} + H^0) \approx -10.0$.

Storey (1981) has calculated rate coefficients α_d for dielectronic recombination of several ions abundant in nebulae. From his results and the entries in Table 7, we find that dielectronic recombination equals or exceeds the combined rates of radiative recombination and charge transfer only for formation of C^+, N^{+2}, and N^{+3}. For these ions, $\log [(\alpha_d N_e/(\alpha N_e + kN_{H^0})] = +0.4, 0.0$, and $+0.4$, respectively. The inclusion of dielectronic recombination will improve the agreement between the observed N^{+3}/N^{+4} ratio and that predicted by Model 2, but it is ambiguous for C^+/C^{+2} and harmful for N^{+2}/N^{+3}.

Storey (1981) also gives line emission coefficients for dielectronic recombination. For the conditions we have derived for NGC 2440, dielectronic recombination ($C^{+2} \rightarrow C^{+1}$) exceeds collisional excitation as a source of emission in C II $\lambda 1335$. The dielectronic recombination contribution is given by

$$\frac{I(\lambda 1335)}{I(\lambda 1907)} = 8 \times 10^{-5} t^{+0.1} e^{7.54/t} . \quad (7)$$

For $t = 1.38$, this gives $I(\lambda 1335)/I(\lambda 1907) = 0.019$, which seems marginally consistent with the limit $I(\lambda 1335)/I(\lambda 1907) \leq 0.013$ that we infer from the *IUE* spectra. This limit suggests that, if Storey's coefficient is correct, the temperature in the C^{++} zone cannot be much lower than the adopted value.

We acknowledge helpful discussions with numerous colleagues, including Harriet Dinerstein, Reggi Dufour, John Scalo, and Mike Werner. Joseph Miller offered useful comments on the manuscript. G. A. S. thanks the Lick Observatory and Board of Studies in Astronomy and Astrophysics of the University of California, Santa Cruz, for their hospitality during the summer and fall of 1980. *IUE* data aquistion and analysis were made possible by support from NASA. Acquisition of ground-based data was supported in part by NSF grants AST 77-21022 to UCLA and AST 78-17836 to Ohio State University. Calculation of some of the models was supported by Academic Computing Service Administration at UCLA. This work was also supported in part by NSF grants AST 78-04575 to the University of Texas at Austin and AST 76-15727 to Ohio State University.

APPENDIX

ATOMIC DATA

a) *Photoionization and Recombination*

For most ions, the radiative and dielectronic recombination coefficients were taken from Aldrovandi and Péquignot (1973). Photoionization cross sections were taken from the compilation by MacAlpine (1971) and Chapman and Henry (1971) and, for higher ions of argon, from Bahcall and Kozlovsky (1968). For sodium, chlorine, potassium, and calcium,

TABLE 9

ADOPTED COLLISION STRENGTHS[a]

Ion	Ω(1, 2)	Ω(1, 3)	Ω(2, 3)	Source[b]
[N II]	2.7	0.35	0.41	S75
[O II]	1.33	0.41	1.71	P76
[O III]	2.36	0.33	0.86	ES
[Ne III]	1.34	0.151	0.24	P74
[Ne IV]	1.10	0.43	1.44	CKSS
[Ne V]	2.08	0.27	0.56	G79
[Na IV]	1.14	0.163	0.157	CKSS
[S II]	7.7	3.0	13.0	P78
[S III]	5.6	1.07	1.39	KC70
[Cl III]	4.9	0.44	1.27	KC70
[Cl III]	3.9	2.1	9.2	KC70
[Cl IV]	2.4	0.37	1.32	KC70
[Ar III]	5.1	0.72	0.89	KC70
[Ar IV]	1.61	0.69	6.0	KC70
[Ar V]	1.27	0.16	1.14	KC70
[K IV]	2.12	0.32	0.84	KC70
[K VI]	0.81	0.11	0.96	KC70
[Ca V]	1.12	0.14	0.83	KC70
C II]		$\Omega(^2P, {}^4P) = 3.1$		J73
N II]		$\Omega(^3P, {}^5P) = 1.3$		J73
N III]		$\Omega(^2P, {}^4P) = 1.9$		J73
O III]		$\Omega(^3P, {}^5S) = 1.22$		BBK*a*
Si III]		$\Omega(^1S, {}^3P) = 5.1$		BBK*b*

[a] Excitation by electron impact at 10^4 K for transition-zone ions and 1.5×10^4 K for other ions. Values from intercombination and permitted lines not listed were taken rom Osterbrock and Wallace 1976.

[b] KEY.—S75, Seaton 1975. P76, Pradhan 1976. ES, Eissner and Seaton 1974. P74, Pradhan 1974. G79, Giles 1979. CKSS Czyzak *et al.* 1967. P78, Pradhan 1978. KC70, Krueger and Czyzak 1970. J73, Jackson 1973. BBK*a*, *b*, Baluja *et al.* 1980*a*, *b*.

we used the semiclassical formulae of Gould (1978) for the threshold photoionization cross sections a_T and the radiative recombination coefficients and assumed $a_\nu = a_T(\nu/\nu_T)^{-2}$, where the ionization potentials $h\nu_T$ were taken from Allen (1973). Recombination coefficients for Cl^0 and Cl^+ were taken from Aldrovandi and Péquignot (1974).

b) Collision Strengths and Transition Probabilities

Transition probabilities for the forbidden lines were taken from Garstang (1968). For the collision strengths, we used the values listed in Table 9, taken from a variety of sources. For the ions taken from Czyzak *et al.* (1967) and Krueger and Czyzak (1970) we have combined the exact-resonance value of Ω^{pp} with the distorted-wave approximation values for the other partial waves (cf. Krueger and Czyzak 1970).

c) Charge-Transfer Coefficients

For Model 1, we used charge transfer coefficients $k = (1.0, 3.0, 1.0, 0.6, 1.5) \times 10^{-9}$ cm^{-3} s^{-1} for (C^{+3}, N^{+3}, O^+, O^{+2}, S^{+3}) reacting with H^0. These values are taken from Blint, Watson, and Christensen (1976), Christensen, Watson, and Blint (1977), Field and Steigman (1977), Butler, Bender, and Dalgarno (1979) and Péquignot, Aldrovandi, and Stasinska (1978), respectively. For N^{+2}, we assumed a rate equal to that for O^{+2} on the basis of empirical indications that N^+ and O^+ have similar ionization functions in nebulae.

REFERENCES

Aitken, D. K., Roche, P. F., Spenser, P. M., and Jones, B. 1979, *Ap. J.*, **233**, 925.
Aldrovandi, S. M. V., and Péquignot, D. 1973, *Astr. Ap.*, **25**, 137.
———. 1974, *Rev. Bras. Fisica*, **4**, 491.
Allen, C. 1973, *Astrophysical Quantities* (London: Athlone Press).
Aller, L. H. 1951, *Ap. J.*, **113**, 125.
———. 1967, *Ap. J.*, **72**, 305.
———. 1957, *Ap. J.*, **135**, 84.
———. 1978, *Proc. Astr. Soc. Australia*, **3**, 212.
———. 1980, preprint.
Aller, L. H., Czyzak, S. J., and Kaler, J. B. 1968, *Ap. J.*, **151**, 187.
Aller, L. H., and Keyes, C. D. 1980, *Proc. Nat. Acad. Sci.*, **77**, 1231.
Aller, L. H., and Walker, M. 1970, *Ap. J.*, **161**, 917.
Bahcall, J. N., and Kozlovsky, B. 1969, *Ap. J.*, **163**, 235.
Balick, B. 1975, *Ap. J.*, **201**, 705.
Baluja, K. L., Burke, P. G., and Kingston, A. E. 1980*a*, *J. Phys. B*, **13**, 829.
———. 1980*b*, *J. Phys. B*, **13**, L543.
Barker, T. 1978, *Ap. J.*, **221**, 145.
Becker, S. A., and Iben, I. 1980, *Ap. J.*, **237**, 111.
Blint, R. J., Watson, W. D., and Christensen, R. B. 1976, *Ap. J.*, **205**, 634.
Bohlin, R. C., Harrington, P. J., and Stecher, T. P. 1978, *Ap. J.*, **219**, 575.
Brocklehurst, M. 1971, *M.N.R.A.S.*, **153**, 471.
———. 1972, *M.N.R.A.S.*, **157**, 211.
Burgess, D. 1967, *Nature*, **216**, 1092.
Butler, S. E., Bender, C. F., and Dalgarno, A. 1979, *Ap. J.* (*Letters*), **230**, L59.
Butler, S. E., and Dalgarno, A. 1980, *Ap. J.*, **241**, 838.
Butler, S. E., Heil, T. G., and Dalgarno, A. 1980, *Ap. J.*, **241**, 442.
Cahn, J., and Kaler, J. B. 1971, *Ap. J. Suppl.*, **22**, 319.
Chapman, R. D., and Henry, R. J. W. 1971, *Ap. J.*, **173**, 244.
Christensen, R. B., Watson, W. D., and Blint, R. J., 1977, *Ap. J.*, **213**, 712.
Cox, D. P. 1972, *Ap. J.*, **178**, 158.
Curtis, H. D. 1918, *Pub. Lick Obs.*, **13**, 57.
Czyzak, S. J., Krueger, T. K., Saraph, H. E., and Seaton, M. J. 1967, *Proc. Phys. Soc.*, **92**, 1146.
Dinerstein, H. 1980*a*, *Ap. J.*, **237**, 486.
———. 1980*b*, Ph.D. thesis, University of California, Santa Crùz.
Eissner, W., and Seaton, M. J. 1974, *J. Phys. B*, **7**, 2533.
Field, G. B., and Steigman, G. 1971, *Ap. J.*, **166**, 59.
Garstang, R. 1968, in *IAU Symposium 34, Planetary Nebulae*, ed. D. E. Osterbrock and C. R. O'Dell (Dordrecht: Reidel), p. 138.
Garstang, R. H., Robb, W. D., and Rountree, S. P. 1978, *Ap. J.*, **222**, 384.
Giles, K. 1979, *M.N.R.A.S.*, **187**, 49P.
Gould, R. J. 1978, *Ap. J.*, **219**, 250.
Harlan, E. A., and Miller, J. S. 1979, *Pub. A.S.P.*, **91**, 168.
Harrington, J. P., and Marionni, P. A. 1980, in *The Universe of Ultraviolet Wavelengths: The First Two Years of IUE* (NASA publication), in press.
Hummer, D. G., and Mihalas, D. 1970*a*, *M.N.R.A.S.*, **147**, 339.
———. 1970*b*, *Joint Inst. Lab. Ap. Repts.*, No. 101.
Jackson, A. 1973, *M.N.R.A.S.*, **165**, 53.
Kaler, J. B. 1966, *Ap. J.*, **143**, 722.
———. 1976, *Ap. J. Suppl.*, **31**, 517.
———. 1979, *Ap. J.*, **228**, 163.
Kaler, J. B., and Aller, L. H. 1974, *Pub. A.S.P.*, **86**, 635.
Kaler, J. B., Aller, L. H., Czyzak, S. J., and Epps, H. 1976, *Ap. J. Suppl.*, **31**, 163.
Keyes, C. D., and Aller, L. H. 1978, *Ap. Space Sci.*, **59**, 91.
Krueger, T. K., and Czyzak, S. J. 1970, *Proc. Roy. Soc. London A*, **318**, 531.
Kwok, S., Purton, C. R., and FitzGerald, M. P. 1978, *Ap. J.* (*Letters*), **219**, L125.
MacAlpine, G. 1971, Ph.D. thesis, University of Wisconsin, Madison.
McCaroll, R., and Valiron, P. 1976, *Astr. Ap.*, **53**, 87.
Mathis, J. S. 1978, in *IAU Symposium 76, Planetary Nebulae*, ed. Y. Terzian (Dordrecht: Reidel), p. 281.
Miller, J. S., and Mathews, W. G. 1972, *Ap. J.*, **172**, 593.
Milne, D. K., and Aller, L. H. 1975, *Astr. Ap.*, **38**, 183.
Minkowski, R. 1964, *Pub. A.S.P.*, **76**, 197.
Morris, M., Redman, R., Reid, M. J., and Dickison, D. F., 1979, *Ap. J.*, **229**, 257.
Nussbaumer, H., and Osterbrock, D. E. 1970, *Ap. J.*, **161**, 811.
Nussbaummer, H., and Storey, P. J. 1978, *Astr. Ap.*, **70**, 37.
O'Dell, C. R. 1963, *Ap. J.*, **138**, 293.
Osterbrock, D. E. 1960, *Ap. J.*, **131**, 541.
Osterbrock, D. E., and Wallace, R. K. 1976, *Ap. Letters*, **19**, 11.
Pagel, B. E. J. 1978, *M.N.R.A.S.*, **183**, 1P.
Peimbert, M., and Torres-Peimbert, S. 1977, *M.N.R.A.S.*, **179**, 217.
Péquignot, D., Aldrovandi, S. M. V., and Stasinska, G. 1978, *Astr. Ap.*, **63**, 313.
Péquignot, D., and Stasinska, G. 1980, *Astr. Ap.*, **81**, 121.
Pradham, A. K. 1974, *J. Phys. B*, **7**, L507.
———. 1976, *M.N.R.A.S.*, **177**, 31.
———. 1978, *M.N.R.A.S.*, **184**, 89P.
Renzini, A., and Voli, M. 1980, preprint.
Ross, J. E., and Aller, L. H. 1976, *Science*, **191**, 1223.
Scalo, J. M., Despain, K. H., and Ulrich, R. K. 1975, *Ap. J.*, **196**, 805.
Seaton, M. J. 1975, *M.N.R.A.S.*, **170**, 475.
———. 1978, in *IAU Symposium 76, Planetary Nebulae*, ed. Y. Terzian (Dordrecht: Reidel), p. 132.
———. 1979, *M.N.R.A.S.*, **187**, 795.
Shields, G. A. 1978*a*, *Ap. J.*, **219**, 565.

Shields, G. A. 1978*b*, *Ap. J.*, **219**, 559.
———. 1980, *Pub. A.S.P.*, **92**, 418.
Shull, J. M., and McCray, R. 1978, *Ap. J.*, **223**, L5.
Storey, P. J. 1981, preprint.
Sweigart, A. V., and Mengel, J. C. 1979, *Ap. J.*, **229**, 624.
Talent, D. L., and Dufour, R. J. 1979, *Ap. J.*, **233**, 888.
Torres-Peimbert, S., and Peimbert, M. 1977, *Rev. Mexicana Astr. Ap.*, **2**, 181.
Whitford, A. E. 1958, *Ap. J.*, **63**, 201.
Williams, R. 1973, *M.N.R.A.S.*, **164**, 111.
Wÿse, A. B. 1942, *Ap. J.*, **95**, 356.

L. H. Aller and C. D. Keyes: Department of Astronomy, University of California, Math-Science Bldg., Los Angeles, CA 90024

S. J. Czyzak: Astronomy Department, Ohio State University, 174 W. 18th Street, Columbus, OH 43210

G. A. Shields: Department of Astronomy, RLM 15.212, University of Texas at Austin, Austin, TX 78712